Performance and cost of field scouting for weeds and diseases using imagery obtained with an Unmanned Aerial Vehicle

ACIDF Project: **2014F171R**

Alberta Agriculture and Forestry

Chris Neeser, Ph.D.
Pest Surveillance Section
403-362-1331 / chris.neeser@gov.ab.ca

Michael Harding, Ph.D.
Pest Surveillance Section
403-362-1338 / michael.harding@gov.ab.ca

Co-applicants:

JZ AERIAL
Jan Zalud
403-259-5006 / jzalud@jzaerial.com

UNIVERSITY OF CALGARY
Schulich School of Engineering
Naser El-Sheimy, Ph. D.
Professor, Canada Research Chair
403-220-7587 / elsheimy@ucalgary.ca

December 2016

Acknowledgements

We would like to extend our sincere thanks and gratitude to Dr. Adel Moussa and Dr. Zahra Lari from the University of Calgary Mobile Multi-Sensor Systems Research Team for their invaluable help with image analysis and pattern detection.

We also like to thank Joe Chomistek, P.Ag. for his assistance with the economic analysis. As well as the following individuals for allowing us access to their fields and providing us with feedback on how they view the value of imagery captured with Unmanned Aerial Vehicles:

- Daryl Chubb (crop consultant)
- Scott Gillespie (crop consultant)
- Spencer Hilton (producer)
- Steve Larocque (producer)
- Don Pederson (producer)
- Karl Slomp (producer)
- Curt Walker (crop consultant)

Finally we wish to thank the Alberta Crop Industry Development Fund and the following producer organizations for their generous financial support:

Executive Summary

Unmanned Aerial Vehicles (UAVs), also known as drones, are increasingly being marketed to farmers and crop consultants as a must have new tool. The promise is that knowledge gained by looking at fields from a bird's eye perspective will enable farmers to better understand yield limiting factors and to take corrective measures where needed. We designed this study with the objectives to examine the value of aerial images captured from a UAV for the purpose of scouting for weeds and diseases in a variety of crops. For each of six crops at two locations, a set of three images (early mid and late season) were taken at 180 m above ground level at a resolution that covered a 6 cm by 6 cm area on the ground for each pixel in the image. This is considered high resolution aerial imagery. However, for the purpose of early season weed scouting we found that this resolution is too coarse to detect the presence of small weeds, which is critical for optimal weed control recommendations. Further testing on much higher resolution images showed that weed density information could be extracted by locating and removing crop rows from the images and then calculating weed density from pixels covering vegetation in the remaining inter-row space. This suggested that it should be possible to use current UAV technology to generate weed density maps without the need to first produce extremely high resolution images of entire fields. Nevertheless the 6 cm per pixel resolution was more than adequate to locate patches that could potentially be associated with disease. We were able to readily detect areas of missing or senescent plants that were less than one square meter in size. Such areas could be identified visually or by the use of segmentation algorithms, but the latter was much more effective in situations where numerous small patches were present throughout the crop canopy. In these cases the algorithm was able to quickly identify thousands of such areas and eliminate the ones that did not meet the specified criteria. Our results support the use of UAV acquired aerial imagery as a new tool to assist with the detection of diseases, especially during the early stages of an infestation. The cost of adding UAV aerial images to a field scouting program is however quite significant. If entirely contracted it could increase crop scouting costs from $4.00 per acre to $40.00 per acre with images taken 12 times during the season. On the other hand if the UAV is farm owned and operated the cost could be much lower, which we estimated at $11.50 per acre. This is primarily because there would be no expectation of profit on the UAV operation as such.

Table of Contents

Introduction

Unmanned Aerial Vehicles (UAVs), also known as drones, are increasingly being marketed to farmers and crop consultants as a must have new tool. The promise is that knowledge gained by looking at fields from a bird's eye perspective, or by examining composite images of entire fields, will enable farmers to better understand yield limiting factors and to take corrective measures where needed. The numerous promotional videos targeted at farmers make it seem quick and easy to capture images and generate field maps, which will reveal areas in need of attention that would otherwise be missed. However, a close look at the technology will show that there are numerous elements that have to work together to produce a field map from a series of images that individually cover only a small portion of a field.

Figure 1. Multirotor and fixed wing UAVs of the type commonly used in agriculture.

Perhaps the first thing is the aircraft itself. It must have the capacity to fly the number of paths required to cover an entire field, typically a quarter section, and maintain its course even under windy conditions. The altitude must be within the limits allowed by Transport Canada and still produce the required overlap between images. The camera has to be triggered at the right time even when travel speed may vary as a result of head or tail winds. UAVs currently marketed for agriculture come in fixed wing or multirotor designs. Fixed wings are better at covering larger areas, such as a quarter section, or in some cases an entire section, whereas multirotors (quadcopters, hexacopters, etc.) are more suitable for small areas and for close up inspections (Fig. 1).

The core piece of technology is without doubt the flight control system. This is what allows the UAV to navigate as programmed, record its position and other flight parameters, as well as to activate the camera or other sensors according to programmed instructions. Autopilots navigate by responding to signals from an onboard GNSS receiver (GPS and/or GLONASS satellites), an inertial navigation system (essentially an accelerometer combined with a gyroscope) and other sensors (altimeter, airflow, etc). Advances in computer technology have increased the accuracy, reduced the size, weight and power consumption, as well as the cost of these systems.

Another critical element is the camera. Many models still use off the shelf point and shoot or action cameras, often modified to capture the near infrared portion on the red band of the digital sensor. Such cameras are of course not optimized for this use and may result in quality and consistency problems with the images. If the camera is not mounted on a gimbal to keep the plane of the sensor parallel to the ground significant distortions may occur especially when subject to lateral wind. In some models the camera may not be adequately protected during landing, resulting in a short lifespan or frequent repairs. Increasingly however, manufacturers offer cameras specifically designed for UAVs. There are now several options for light weight and relatively low cost multispectral cameras, thermal infrared

Figure 2. A ground telemetry module (GTM) connected to a laptop with a screen shade. The laptop runs the flight planning software and displays the position, altitude, speed, battery status and other information relevant to the operation of the UAV.

cameras, and even compact LIDAR units. In many cases these cameras are now mounted inside the fuselage and protected from dust and debris, which is often a problem with small fixed wing UAVs during landing.

Once airborne the UAV communicates with the operator through a radio, known as the ground telemetry module (GTM). This allows to display the position of the UAV on the flight plan, to show flight parameters, such as altitude, speed and battery status, as well as to stream video and other information related to payload sensors. When necessary, the operator has the option to switch to manual flight control using the remote control radio unit (Fig. 2 and 3). In some cases the GTM and the remote control radio are integrated into one unit. This setup often relies on a tablet computer or smartphone to provide processing power to display digital video and to handle other computational tasks associated with the flight planning software.

The introduction of visual flight planning software that allows the user to specify waypoints by clicking on a map has greatly simplified the flight planning process. No longer is it necessary to enter coordinates for waypoints or to calculate the distances between paths to achieve sufficient overlap. What previously might have taken hours of preparation can now be achieved in minutes. In many cases the flight plan can be overlaid onto a variety of base maps, including satellite imagery, which often makes it easier to find reference points and to locate good areas for field set-up. The software may also include features for calibration of the camera and other sensor as well as to carry out pre-flight checks.

Figure 3. UAV operated via manual controls using a 2.4 GHz Spectrum DX7 controller.

Once the information has been collected it needs to be processed. Typically the task consists in creating a single image of the entire target area by combining the set of overlapping images, which is referred to as mosaicking. Finally the mosaicked image has to be adjusted to remove any distortions and geographic coordinates have to be assigned. The result is an orthoimage that has a consistent scale in all areas and can readily be placed on a map within a geographic information system. Depending on the number and size of the image files involved, this can be very

computationally intensive task that relies on specialized software. The resulting image can then be further analyzed, for example to generate a normalized difference vegetation index (NDVI). The orthoimage can also be subjected to a number of analytical methods to characterize and extract patterns. In order to efficiently analyze spatial information it is necessary to organize the images and files derived from them, into a geographic information system (GIS). GIS software allows to display, organize and analyze such data in an efficient manner.

Crop scouting with UAVs has been proposed as a potentially valuable application of UAV technology. The capture of high resolution images at very low altitudes suggest that images could be used to detect weeds and diseases that produce visual symptoms in the crop canopy (Peña-Barragãn, Castro-Mejías et al. 2013, Baranowski, Jedryczka et al. 2015). Although theoretically plausible such an application needs further evaluation to gain a better understanding of current limitations and developments required. We designed this study with the objectives to examine if UAV technology, as it is currently being marketed for on farm use, provides useful information for field scouting of weeds and diseases.

Protocol

In April of 2014 we located two fields of each of the following six crops: barley, canola, field peas, potatoes, seed alfalfa and spring wheat. The fields were located in southern Alberta and spread over four counties, namely the county of Newell, Wheatland, Kneehill and Starland. Images of the fields were captured at three occasions during the growing season, ranging from May 26 to June 22, from July 16 to August 1 and from August 10 to September 7. The dates were chosen according to developmental stages of the crops (Table 1.). The intent was to obtain a set of images early in the season, prior to pots-emergence herbicide applications, to evaluate their usefulness for weed detection. Whereas the purpose of the second and third set was to assess their potential for locating crop diseases.

Table 1. A list of the dates at which the aerial images were taken. All images were taken in 2014 and there were two fields for each crop.

Crop	Capture 1	Capture 2	Capture 3
Alfalfa	May 28, 31	July 22	Aug. 18
Barley	May 26	July 16	Aug. 15
Canola	June 2, 6	July 27, 29	Aug. 19, Sept. 4
Peas	June 5, 6	July 29, Aug. 1	Aug. 10, 19
Potatoes	June 22	July 22, 31	Aug. 10, Sept. 7
Wheat	June 3, 6	July 27	Aug. 27, Sept. 4

The equipment to capture the images consisted of a custom built fixed wing airframe (Fig. 4) equipped with a MicroPilot[1] MP2028 flight control system and ground control software. Communication with the computer on the ground was through an XTend-PKG telemetry unit. The UAV had a 127 cm fuselage, a 183 cm wingspan and weighed 2,800 g including the payload. When not in autopilot mode, during landing, it was piloted remotely with a 2.4 GHz Spectrum DX7 controller[2].

Figure 4. The custom build fixed wing UAV that was used for this project. It is equipped with a MicroPilot MP2028 flight controller, has 183 cm wingspan and weighs 2800g with camera payload.

The camera was a Canon PowerShot SX260 HS, in which the near infrared filter had been replaced with a filter to capture radiation in the red portion of the electromagnetic spectrum and allow the CMOS sensor to record the near infrared (700-1000 nm) portion of the spectrum. Individual images contained 12 million pixels (3000 px by 4000 px) at 24 bits per channel and were stored in jpg format. The images, which were taken at 180 m above ground level, covered a 6 cm by 6 cm area on the ground for each pixel in the image. This is also referred to as a 6 cm ground sampling distance (GSD).

[1] https://www.micropilot.com
[2] http://www.spektrumrc.com

Flight plans for the quarter section sized fields had 10 to 12 passes for a total of 110 to 140 images per field. These images were combined into a single image using AgiSoft[3] and EnsoMosaic[4] software. At least five ground control points were located along two or three boundaries of each field to serve as reference points. The location of the ground control points was measured with a handheld Ashtech Mobile Mapper[5] GNSS unit with an expected accuracy of +/- 0.1 m. The ground control point markers consisted of a 1 m^2 piece of white tarp marked with large black X.

Ground level reference observations were conducted in all fields following the capture of each set of aerial images. Points of interest were chosen from the aerial images and located in the field using the Ashtech GNSS unit. Once located, a 1 m^2 PVC frame was placed on the ground, within which disease incidence and weed populations were assessed. A picture from a vertical position directly above the sample plots was taken. In this case we used a remotely controlled DSLR camera (Canon EOS Digital Rebel XTi) mounted on a 2.5 m pole with a horizontal arm. This setup was also used to collect additional images during early stages of crop development to further analyze the feasibility of detecting small weed seedlings.

The orthorectified and geotagged mosaics were imported into ArcGIS[6] for analysis and to generate images of a modified Normalized Difference Vegetation Index (NDVI). The NDVI provides a way to standardize pixel values to a range of values falling between -1 and +1. They are calculated as follows:

$$NDVI = \frac{NIR - R}{NIR + R}$$

where R stands for pixel values in the red channel and NIR stands for pixel values in the near infrared channel. The resulting image has single grey scale channel which can be mapped to any arbitrary set of colors, for example, so as to highlight certain ranges of values that may represent a feature of interest.

We used a modified version of this index to accommodate for the fact that our camera did not offer the option to record in the infrared and red channels at the same time. This is of course a limitation on all cameras intended for normal photography. Instead we used the following modified version:

$$NDVI_m = \frac{NIR - B}{NIR + B}$$

where B stands for pixel values in the blue channel. Replacing the red channel with the blue is the most commonly used modified NDVI in images acquired with UAVs for agronomic purposes UAV (Rasmussen, Ntakos et al. 2016).

[3] http://www.agisoft.com
[4] http://www.mosaicmill.com
[5] http://intech.trimble.com (Ashtech was acquired by Trimble who is no longer selling the Ashtek Mobile Mapper series of GNSS units)
[6] http://www.arcgis.com

Additional image processing and analysis was done with imageJ[7], Matlab[8] and to some extent with Adobe Photoshop[9]. The open source imageJ software was used primarily for image segmentation and object analysis, whereas Matlab was used to develop the algorithm used to locate crop rows and also to conduct image segmentation. Adobe Photoshop was used for resizing and reformatting, as well as for lightness and contrast adjustment.

Usefulness of Images for the Detection of Weeds

Field scouting for weeds is most useful in the spring before the application of herbicides, which can be prior to seeding, after seeding or both. In either case weeds will be small and occupy only very little of the available space. The extent to which individual weed seedlings register on the sensor of a camera depends on the ground sampling distance. As the ground sampling distance increases the contribution to the image of the light reflected by a small object decreases. This is illustrated in figure 5, with a stinkweed seedling shown at a ground sampling distances of 0.01 cm, 1.0 cm and 6.0 cm. At 0.01 cm/pixel the color and shape of the seedling is readily distinguished from the background, at 1.0 cm/pixel the green color of the foliage is still being registered, but the shape is no longer distinguishable. Finally at 6 cm/pixel the color reflected from the seedling has only a small impact on the color of the pixel, and is no longer distinguishable from the background. Consequently the field images we captured at a ground sampling distance of 6 cm are not suitable to detect individual weed seedlings. However this is not to say that larger weeds, or patches of weeds could not be detected.

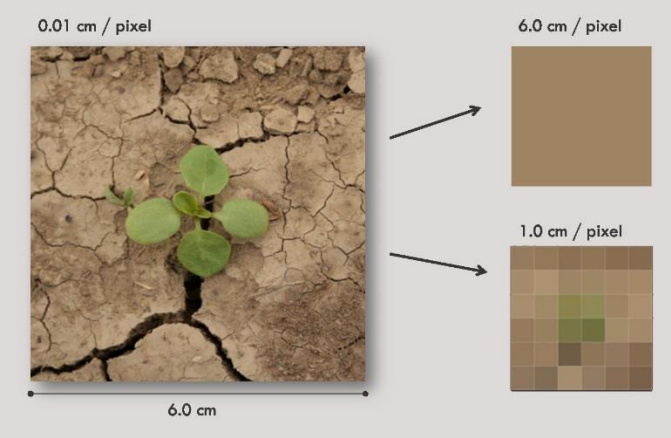

Figure 5. Visibility of a small seedling on images with different ground sampling distances (GSD). At a GSD of 6 cm the seedling can no longer be distinguished from the background. The GSD is the distance covered on the ground by the width of one pixel.

To further explore the weed detection potential of our aerial images recorded at a 6 cm GSD, we selected representative samples of images taken at a high resolution for ground truthing and down sampled them to the equivalent of 6 cm ground sampling distance. Then we overlaid the outline of crop rows and of weeds onto these images (Fig. 6) and calculated the proportion of background pixels, those covering soil and crop residues, that were not distinguishable from pixels covered with vegetation. We found that in four out of the six crops more than 80% of the pixels that were in fact background were not distinguishable from vegetation. The difference between background and vegetation was more pronounced in canola, where 61 % of the pixels were ambiguous and most well defined in potatoes were only 16 % of the background pixels could not be distinguished from vegetation.

[7] https://imagej.nih.gov/ij
[8] https://www.mathworks.com/products/matlab/
[9] http://www.adobe.com/ca/products/photoshop.html

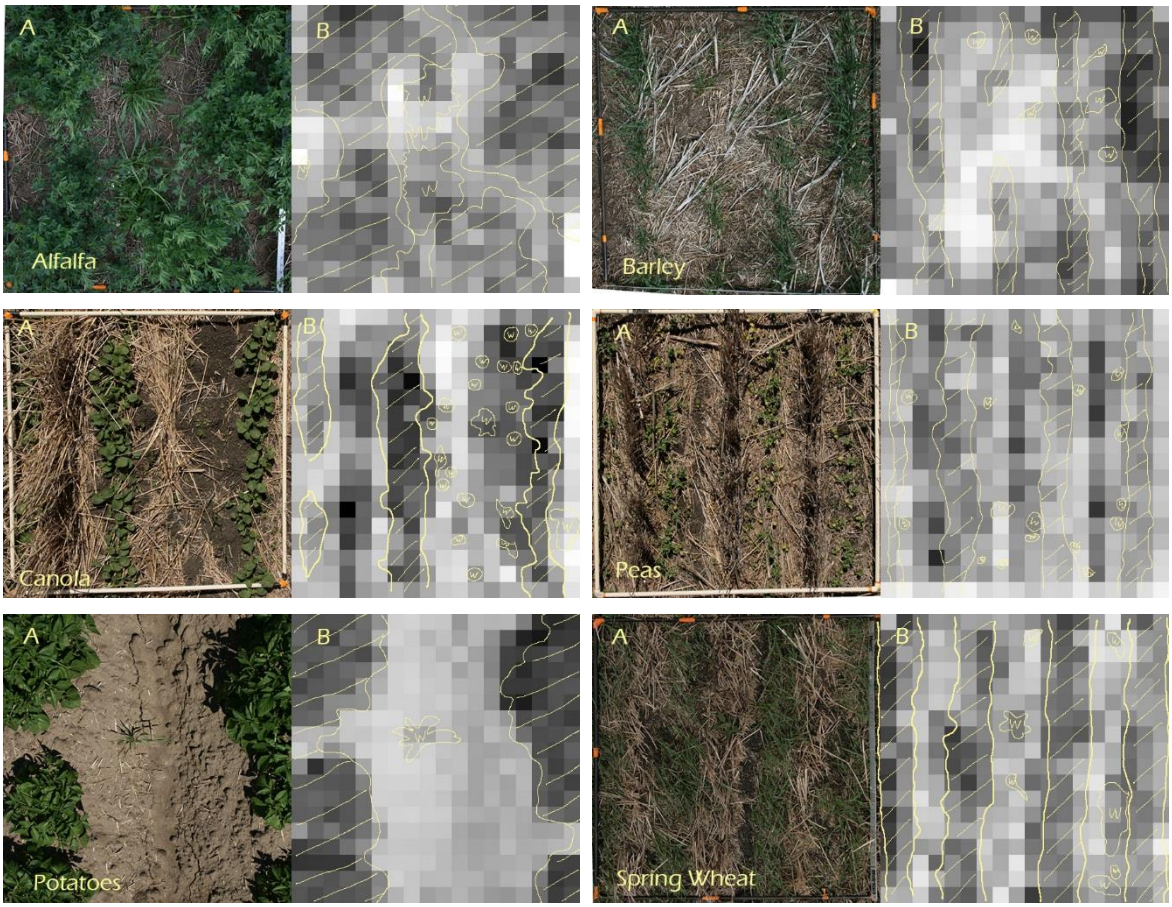

Figure 6. Limitations of image resolution on the ability to distinguish growing vegetation from the background. For each crop (A) the corresponding 6 cm ground sampling distance (GSD) gray scale image (B) is shown with vegetated areas outlined in yellow. The proportion of background pixels (free of vegetation) that on the 6 cm GSD image could not be distinguished from pixels with actively growing vegetation were as follows: 89% for alfalfa, 86% for barley, 61% for canola, 86% for peas, 16% for potatoes and 82% for spring wheat.

If we had used a more advanced analysis that would have combined data from all three channels of the color images, it is likely that we could have reduced the proportion of ambiguous pixels, but probably not to the point that would allow reliable detection of weeds, especially when they are not clumped together. We did however, examine the $NDVI_m$ values of pixels within the quadrats that were selected for ground truthing, and for which weed cover was measured. The correlation results for weed cover and the corresponding $NDVI_m$ values are presented in table 2. In barley, canola and peas the correlation was not significant. It was significant in alfalfa and wheat, while only marginally so in potatoes. The strength of the correlation is most likely related to the total weed cover. The correlations were strongest in those crops where the ground truthing quadrats had the highest weed cover (Fig. 7).

In view the above findings it appears that for the purpose of weed scouting the images have to be of a much higher resolution. The problem with increasing the image resolution is that it also drastically increases the size of image files per unit area of terrain covered. For example, decreasing the ground sampling distance from 6 cm to 1 cm would increase the number of pixels by a factor of 36. A typical orthoimage of a quarter section that may occupy 350 MB at the 6 cm GSD would increase to 12.2 GB at

1 cm ground sampling distance, therefore making it challenging to process with ordinary computer systems. This problem can be avoided if images are processed as they are captured and only the extracted information is retained. We tested the feasibility of this approach on a set of images taken at a height of 2.5 meters with the objective to determine percent weed cover within each image. Ultimately this approach could be used to generate a weed density map on the basis of percent weed cover values extracted from images that only represent a sample of the entire field.

Table 2. Correlations between ground cover of weeds and the corresponding average NDVI values. Weed cover was estimated visually for each ground control plot whereas the NDVI values were derived from the aerial images. Low chi-square values (<0.05) indicate statistical significance.

Crop	Sample	Pearson's r	Chi-Square test
Alfalfa	24	0.51	0.01
Barley	21	0.26	0.25
Canola	24	0.10	0.64
Peas	24	0.04	0.85
Potatoes	24	0.37	0.07
Wheat	23	0.74	<0.01

The primary challenge in determining weed cover is to separate pixels with vegetation into crop and weed categories. Given the diversity of crops and weeds it is not likely that this can be achieved on the basis of spectral patterns of reflectance. Instead we propose to determine weed cover by considering only the space not occupied by crop rows. The process consists of locating the crop rows within the image, then removing from the analysis pixels that a part of the crop rows by assigning them a value that is out of range (black or white) and finally determining the proportion of pixels that show living vegetation in the remainder of the pixels.

To locate the crop rows we used a technique known as the Hough transform, to find linear features within the image (Dlouhy, Lev et al. 2016). The five highest candidate linear features were then tested for consistency in their orientation angles. For each candidate angle and for each candidate row count a fit score, which assumed a fixed row distance, was calculated. A fit score was calculated for a range of possible row offsets from the image border as well as orientation angles. The row location and row angle was then selected on the basis of the highest fit score. The remaining rows were located on the assumption of a fixed row spacing and parallel orientation, using discrete optimization criteria. Finally for each row, a sliding window was searched around the center line to locate the row boundary, so as to include at least 95 % of the vegetation at any location of the sliding window. The resulting row boundaries were straight lines with no attempt made to account for variations

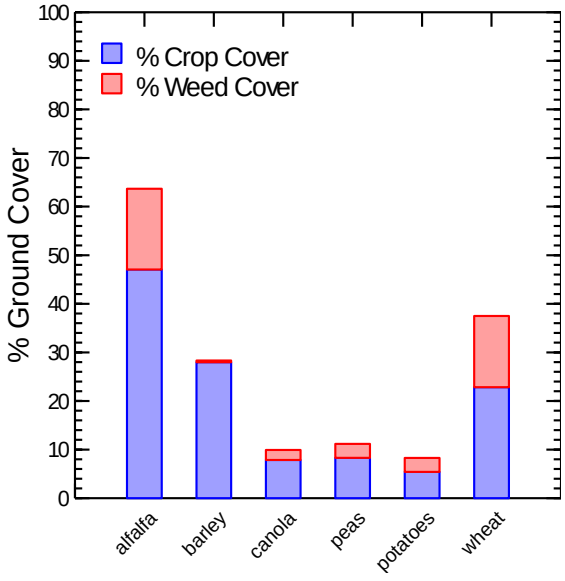

Figure 7. Percent ground cover of weeds and crops within the 1 m² quadrats established as ground control points for each crop.

in row width. The algorithm was tested on 9 sample images of wheat ranging from growth stage 1 to 3 and 6 sample images of barley ranging from growth stage 1 to 5 on the Feekes scale of cereal growth. The algorithm was found to work quite well, correctly locating 96 % of the crop rows (Fig. 8). Problems occurred in a few cases where the assumptions of parallel and/or equally spaced rows were violated.

Figure 8. Delimitation of crop rows with the Hough algorithm.

The performance of the row detection algorithm to calculate the percentage weed cover in the space not occupied by crops was tested by comparing weed cover calculated from visually delimited inter-row space to weed cover values obtained when crop rows were treated as bands with straight borders (Fig. 9). The calculations were done on 16 grey scale images using only the red band. The results showed that aside from three exceptions the differences in percent weed cover obtained from the manual or automated methods were small (Fig 10). However even with the exceptional values included the t-test is not significant at the 10% probability level. Consequently it appears that treating crop rows as bands with straight borders does not lead to less accurate estimates of weed cover.

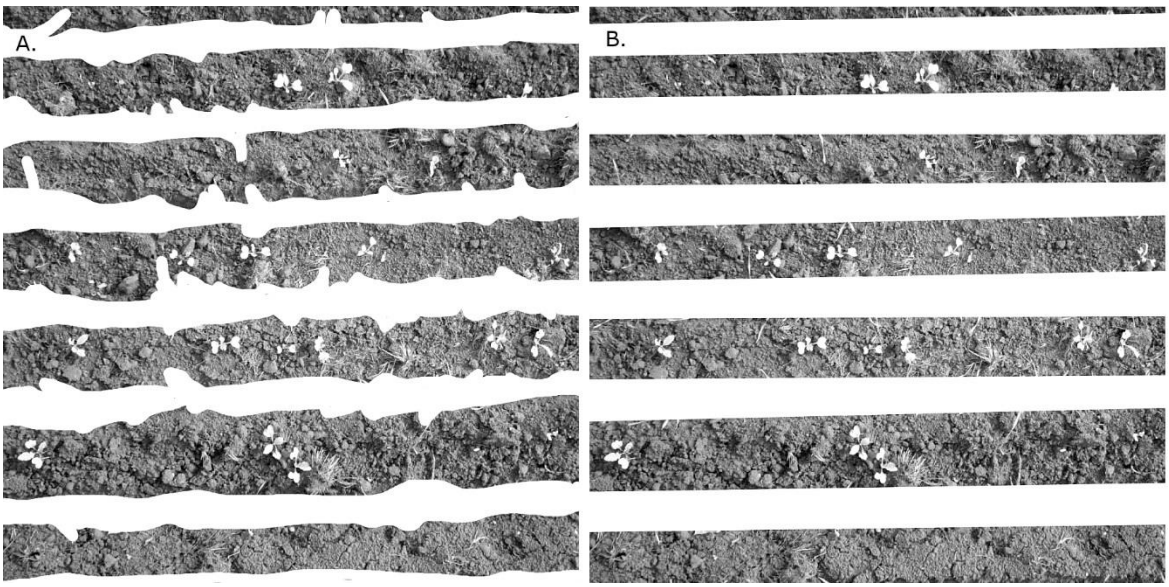

Figure 9. Inter-row space delimited by crop rows with irregular shaped edges(A.) and inter-row space delimited by crop rows with straight edges (B.). The weed density was calculated as the percentage of pixels occupied by vegetation relative to the total number of pixels in the inter-row space.

From the above we can conclude that in principle it should be feasible to photographically sample fields in a systematic fashion and to process these images to extract weed coverage values. These data points can then be interpolated to generate a weed coverage map. Such maps would only require minimal

computing resources for display and could readily be processed for use in precision farming. However, because of the often patchy distribution of weeds and the relatively small size of typical weed patches, the sampling interval has to be small enough to capture patches that may only be a few meters wide (Gold, Wilkerson et al. 1996). Therefore sampling density and the dimensions of the area covered by each sample will have to be optimized to obtain a map that is sufficiently accurate. As a general rule we can anticipate that the distance between samples has to be less than the width of the weed patches that are to be detected and the area covered by each image will also have to conform to this scale (Krueger, Wilkerson et al. 2000). Consequently, an accurate weed density map that can resolve patterns in the 10-20 meter range will require a large number of sample points per field. For example, to cover a quarter section on a 5 m grid 25,600 sample points would be needed. Capturing and processing this many images certainly poses a technological challenge beyond the capacity of low cost UAV's. Fortunately the problem can be circumvented by extracting multiple sample points from single images. An image that covers 20 by 20 meters on the ground could be used to obtain at least 25 sample points, each averaging the weed cover for a 4 m^2 section. In this way the number of images and flight passes across the field could be drastically reduced, bringing it within the range of current UAV technology available for on farm use.

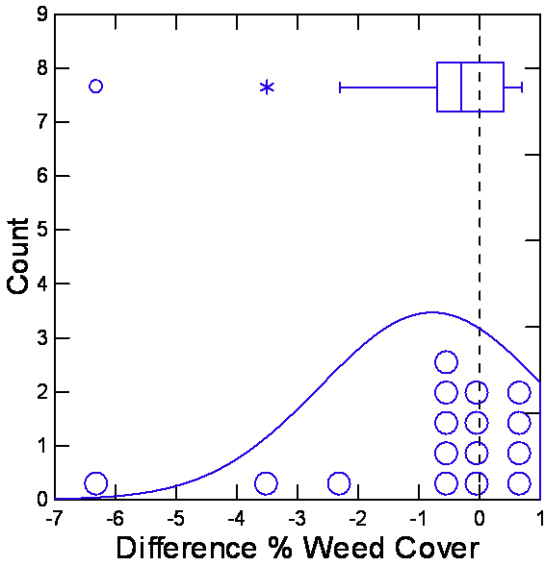

Figure 10. The difference in percent weed cover in 16 sample images, where weed cover estimates obtained on the basis of rectangular inter-row sections were subtracted from estimates where weed cover was calculated on the basis of irregularly shaped, visually defined inter-rows. When all three extreme values are included the t-test gives an 11 % probability that there is in fact no difference between the two methods. Without the three extreme values this probability increases to 83 %.

Usefulness of Images for the Detection of Diseases

Many plant diseases result in the formation of patterns that are visible when a crop canopy is viewed from above. These patterns reflect the presence of unhealthy plants, but without necessarily revealing any specific symptoms. The reason that distinct patterns can be observed is because infections are more likely to spread to neighbouring plants than to plants further away, therefore producing visible patches in the crop canopy. Depending on the virulence of the disease such patches will grow more or less rapidly and merge with other patches in the vicinity (Evans, Baierl et al. 2003, Isard and Chamecki 2016).

However, not all patches that appear in a crop canopy are due to disease. In fact there are numerous causes that will produce some kind of visible mark on a crop canopy. Some of the common undesirable patterns we observed were due to seeding problems, vehicle traffic, accumulation of crop residues, poor drainage and soil conditions (Fig. 11). Fortunately patterns in the crop canopy that are produced by diseases tend to have characteristics that can be distinguished from patterns that have other causes

(Clark 1990). Diseases tend to spread radially, therefore producing circular or oval shapes without the linear features that are produced by mechanical equipment.

It is therefore possible to assign criteria that could be used to eliminate patterns that are unlikely to be caused by disease and select those that are for further inspection. Table 3 describes several commonly used measures to quantify the shapes of two dimensional objects. Individually or in combination these measures can be used as numerical sieves to remove objects based on specific shape criteria. Using this technique we were able to easily remove tracks and rectangular patterns that were produced by farm equipment.

We also found that the orthoimages that we produced were sufficiently accurate to locate even small patches. We were able to transfer the

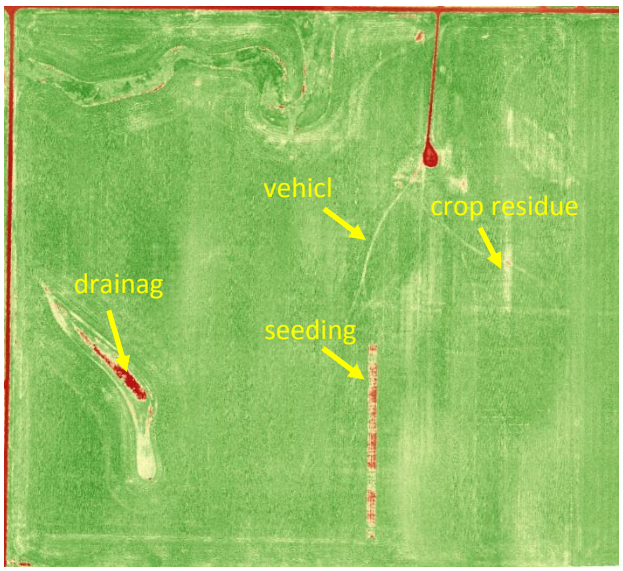

Figure 11. Crop canopy patterns readily distinguishable from potentially diseased areas. Such patterns exhibit shapes or are associated with locations that discard the possibility of plant disease.

Table 3. Common measures to describe simple two dimensional geometric patterns, their formula and values for a range of typical shapes.

Shape	Aspect Ratio	Circularity	Roundness	Eccentricity	Rectangularity
	$= \frac{major\ axis}{minor\ axis}$	$= \frac{4 * \pi * area}{perimeter^2}$	$= \frac{4 * area}{\pi * major\ axis^2}$	$= \sqrt{1 - \frac{(0.5 * minor\ axis)^2}{(0.5 * major\ axis)^2}}$	$= \frac{\frac{\pi}{4} ab}{H * W}$ *
	1.00	1.00	1.00	0.00	0.78
	1.50	0.85	0.67	0.75	0.78
	1.00	0.79	1.00	0.00	1.00
	2.00	0.70	0.5	0.87	1.00
	1.13	0.80	0.89	0.46	0.80
	1.86	0.71	0.53	0.84	0.68

*where **a** is the major axis and **b** is the minor axis of a two dimensional shape, H is the height and W with the width of the bounding rectangle.

coordinates from the images and consistently find these locations on the ground using our handheld GNSS unit. The most basic application of UAV generated images could therefore consist in examining the field mosaics or the derived NDVI images and locate patches that suggest the presence of infected plants.

Given that a detailed visual inspection of a large image (500 MB) is very time consuming, it would be advantageous to automate the process of locating potentially infected areas. This can be achieved by segmenting the images to assign certain values to regions of greater similarity and subsequent filtering so as to retain only those patterns that match a given set of criteria. To this effect we used a trainable segmentation algorithm that relied on samples of the patterns of interest to locate similar patterns. To avoid unnecessary complexity, image areas not part of the area under cultivation (road allowances, sloughs, buildings, etc.) were masked and therefore removed from the analysis. A mask is a binary or greyscale image that delimits the areas to be included for further processing. Once created a mask can be reused for the same field as long as the surface under cultivation remains unchanged.

We found that the number of patches of interest within a field can vary considerably. This depends on the crop and the characteristics of the patches that are being searched for. For the purpose of discovering potentially diseased areas we examined the mosaics of the images taken mid-season, with capture dates ranging from July 16 to August 1.

The alfalfa images revealed distinct patterns that were the result of localized drought stress, which was confirmed by field inspection of these areas (Fig. 12). The problem could have been due to deficiencies in the irrigation equipment (center pivots), to differences in the water holding capacity of the soil, or a combination of both factors. In this case the patches were fairly large and readily identifiable from a visual inspection of the image, even when zoomed out to a much lower resolution than the original. It is noteworthy that the algorithm was able to largely ignore the effect of the shading produced by the clouds, which was not easily achieved by visual observation.

In the case of the barley fields the images were again dominated by a smaller number of large patches with fairly irregular shapes (Fig. 13). These images were taken on July 16 at a time when the crop canopy had already started to senesce. Ground truthing revealed that these patches reflected more advanced crop maturity and that there was a certain amount of foliar disease present, but this appeared to have had a minor impact compared to variability in crop maturity. We concluded that other factors, such as differences in soil and landscape position were most influential in the patchiness that we observed. This finding highlights the importance of timing and the constraints this presents to anyone aiming at covering a large number of fields.

The segmentation of the canola fields produced a very different pattern. This time there were numerous small patches more or less oval in shape (Fig. 15). In the field shown in figure 15 A., the patches tend to align with the crop rows, which was not the case in the other field where no distinct rows were present, because it had been seeded in two passes at right angles. The selection algorithm excluded track marks, seeding misses and areas with bare soil, but attempted to capture areas that had a reduced amount of vegetation compared to their surroundings. Such patches could be the result of disease or other causes. For this project we did not have the resources to do a comprehensive survey to investigate individual patches. Nevertheless, it is likely that a map of patches with reduced vegetative cover has the potential

to greatly increase the likelihood of detecting diseased canola plants. Instead of randomly sampling the entire field, the map allows to concentrate on areas with a high likelihood of the presence of diseases,

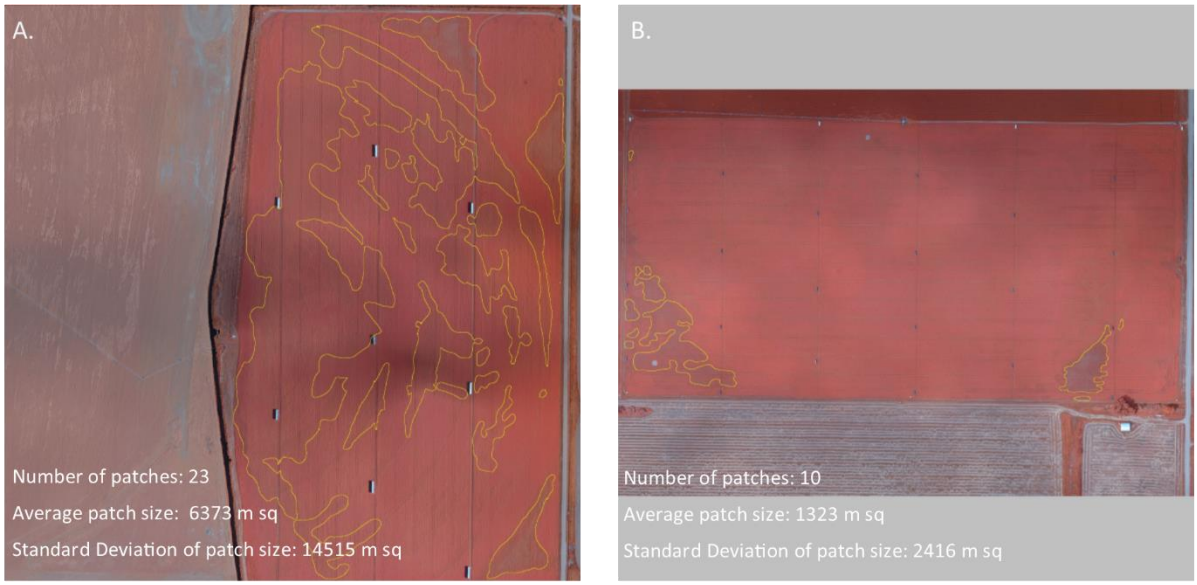

Figure 12. NIR images of two irrigated seed alfalfa fields taken on July 22, 2014. Image segmentation was able to successfully discriminate between shading caused by clouds (especially visible in the centre of image A.) and areas with poor growth, which were due to sub-optimal delivery of irrigation water. Diseases that produce patterns in the canopy visible from above were not observed in either one of these fields.

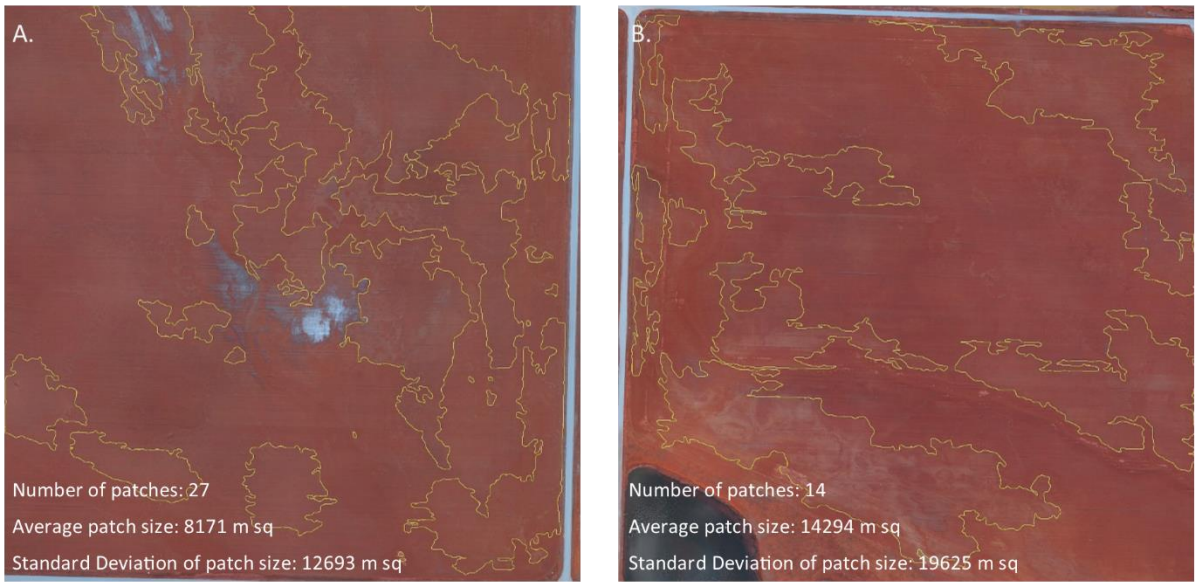

Figure 13. NIR images of barley fields taken on July 16, 2014. In both cases the segmentation algorithm was able to separate areas of reduced growth from sloughs and areas not suitable for crop production. This is especially obvious with the grey water logged areas in image A. where no crop was present.

Figure 14. NIR images of two canola fields taken on July 27 (A.) and July 29 (B.) of 2014. The segmentation isolated numerous small patches and was largely able to discriminate between patterns caused by machinery and patches resulting from other causes. The segmentation parameters were adjusted to extract small patches with a generally round or oval appearance.

Figure 15. NIR image of two pea fields taken on Aug. 1. (A.) and July 29 (B.) of 2014. For these fields the segmentation focused on patches with higher values in the NIR band (red) because, unlike in other fields at this time, here the lower values formed the background (one large connected area). Overall in this case the segmentation algorithm used did not work as well as with other crop canopy images taken at mid-season.

such as clubroot, blackleg, verticillium, etc. This is especially true when affected areas are small and unevenly dispersed. As for example in figure 14-A. where 1073 patches occupied only 5900 m^2, which corresponds to 0.9% of the total field area. If one were to randomly sample this field with non-overlapping 1m^2 quadrats at least 200 samples would be needed for a 50% chance of capturing one or more of the areas marked as a patch (assuming a binomial distribution). In other words detecting things that occur in small patches distributed across a large area, requires a large number of samples if a random approach is used. If instead we can target the sampling towards areas with a higher probability of presenting the condition that we are trying to detect, the sampling can be substantially reduced. This may be especially useful for the early detection of relatively slow spreading soil-borne diseases.

When the segmentation was applied to the pea fields, which were taken on August 1 (Fig. 15 A.) and July 29 (Fig. 15 B.) we found that the patches were formed by the more vigorously growing areas, while the areas that had lower NIR values (less red) were more or less merged together into the background. Again the algorithm was fairly effective at separating the effect of shading by clouds from the crop canopy. Similarly to the barley fields in figure 13, the patterns in the pea canopy reflect the onset of senescence, which appears to be influenced by soil related patterns. This shows that crops can be quite variable within a field, which is most likely also reflected in the yield distribution.

The two potato fields in figure 16 exhibited distinct variety dependent canopy characteristics. The cultivar in Field A. had an open canopy with substantial bare space not covered by the crop canopy between crop rows. While the cultivar in field B had a completely closed canopy. Not only did the cultivar in field A produce less foliage, but it also began to senesce much earlier. In fact the segmentation of this field captured a very large number of small patches defined by NIR values that were intermediate between healthy vegetation and bare soil. The segmentation method used was effective at locating problems specific to the canopy and ignoring inter-row space and other areas not occupied by the crop. Individual patches do not necessarily indicate disease, but they present a much reduced subset of the whole field that could be subjected to further analysis and subsequent field sampling.

In field B the patches were of a different nature, again much larger and fewer in number. They were for the most part readily visible when zoomed out and appear to reflect patterns determined by soil conditions. In fact most of the larger patches were associated with excessive soil moisture. Although no specific disease problem could be identified, the areas delimited by the segmentation suggest crop stress that may favour the development of disease. As such the image could be useful for monitoring or for long term field management.

The two fields of spring wheat presented different types of problems. Field A shown in figure 17 had areas with lodging and also areas with reduced stand density. The lodging was in some areas difficult to delimit because it could at times taper of gradually without a clear border. The drainage channel and the access road on the north end, as well as the slough in the south western section of the field were masked out as permanent non-crop features. However the unseeded strip in the southern portion was removed by the segmentation because it fell outside of the color and shape criteria. In this case the observed patches were not indicative of disease, but instead may point to higher levels of available nitrogen where lodging occurred.

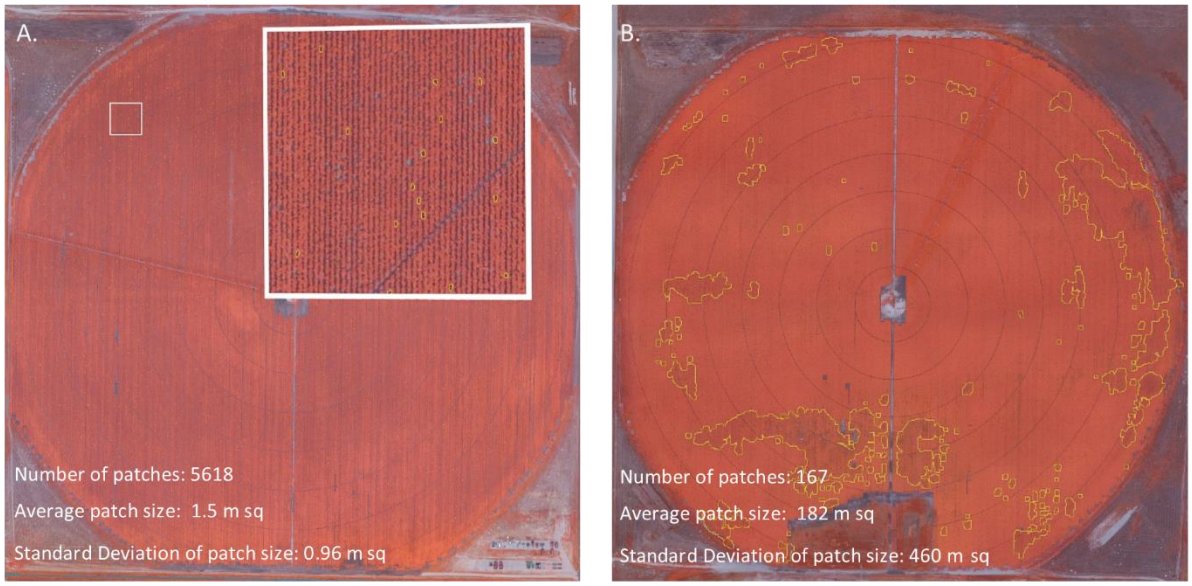

Figure 16. NIR image of two potato fields taken on July 22 (A.) and July 31 (B.) of 2014. The segmentation in field A identified a large number of small patches that were generally confined to a single row. The algorithm performed fairly well in separating bare soil, due to incomplete canopy cover between crop rows, from partially exposed soil resulting from dieback in the canopy or other causes. Seeding misses and other patterns linear patterns (irrigation tracks) were also readily ignored. Field B presented a very different picture since there was complete canopy cover producing larger patterns similar to what was observed in other crops.

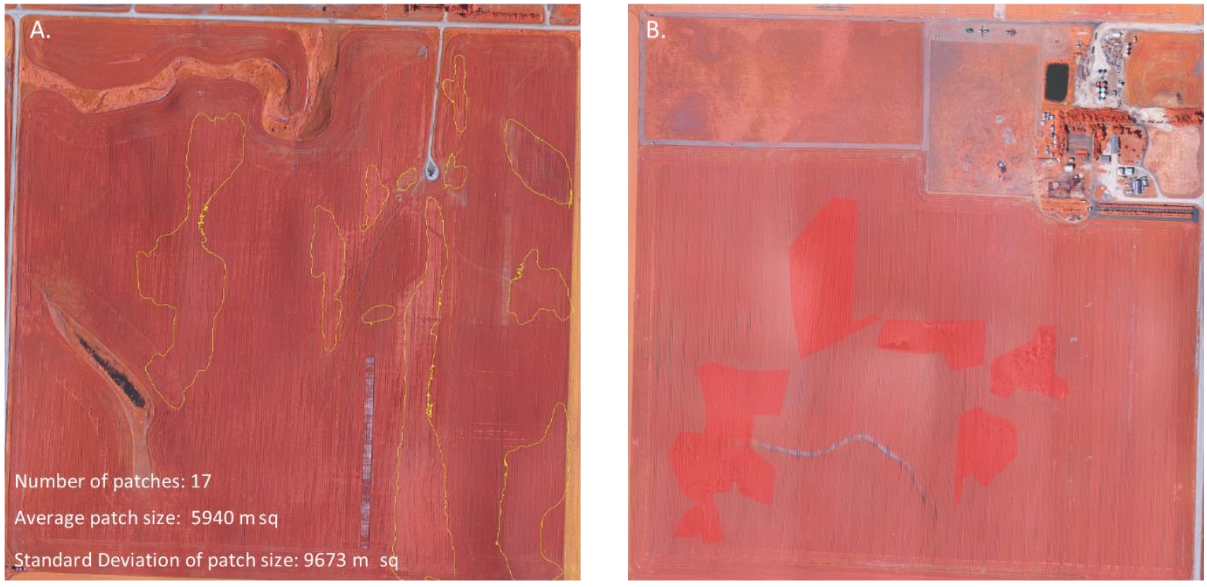

Figure 17. NIR images of two spring wheat fields taken on July 27, 2014. Field A had areas with lodging that showed as lighter colored patches whereas other areas were darker. Sloughs and natural drainage channels were excluded from the analysis. The image of the second wheat field (B) had a number of areas where the stitching process failed (highlighted areas), presumably due to the uniform appearance of the canopy at the time the pictures were taken.

The wheat field in figure 17 B, consisted of a very uniform stand with no obvious patches at the time the image was captured (July 27). The lack of well-defined patterns within the field area made it difficult to correctly assemble the mosaic. The problem areas were highlighted in red. It can also be seen that there are four vertical bands, which are an artefact stemming from image capture, possibly due to light reflecting from the side of the UAV into the camera lens, which was mounted under the wing. Although there were problems in important areas of this image there was enough detail in other areas to reveal modest damage caused by deer.

In the case of wheat and barley during ground truthing we also collected ten flag leaves within each sample area. The amount of foliar disease (leaf spots) was rated using a modified Cobb scale and averaged for each sample. We tested if there was a correlation between disease ratings and the average $NDVI_m$ value from which the leaves were taken. But there was in fact no correlation (Fig. 18). This result was not unexpected because as already mentioned, much of the barley crop had already began to turn yellow and had stopped photosynthesizing and there was little foliar disease in the wheat fields. Any effect caused by leaf spots was drowned out by the overall loss in photosynthesis.

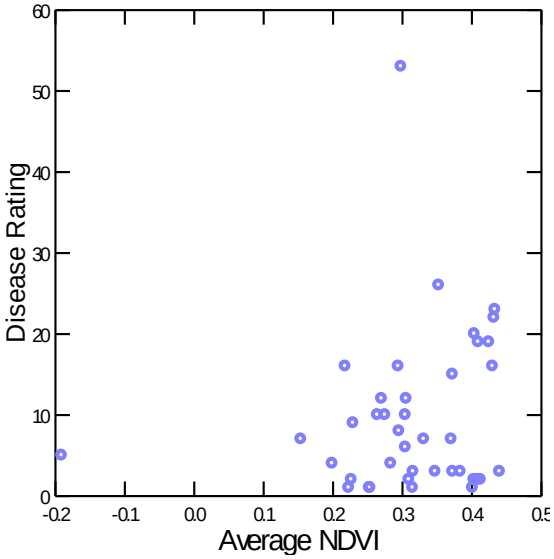

Figure 18. Absence of correlation between $NDVI_m$ and disease rating (modified Cobb scale) on flag leaves of barley and wheat.

Our results show that image segmentation can be effective at identifying patches in a crop canopy that could be caused by disease. The algorithm used worked with a wide range of patch size and distribution patterns. It was also capable of ignoring patches that were likely related to field operations, such as vehicle tracks and seeding misses. However, the presence of patches does not imply the presence of disease. Therefore additional verification is required, which could consist of visual inspections, additional UAV based close-up photography with manual or automated diagnostics, or the use of a UAV to collect samples. When the number of suspect areas is small, then in-person visual inspection is probably the most efficient way to proceed. UAV based solutions would be most beneficial when there are a large number of patches with a low probability of being positive for a particular disease. Automated navigation to capture images at close range at multiple locations within a field, is now within the capability of current UAVs (Dlouhy, Lev et al. 2016). The automated recognition of disease symptoms has been demonstrated for citrus black spot (*Guignardia citricarpa*) on oranges, where object recognition (isolation of shapes) and spectral signatures were combined to achieve accuracies of 96 % (Bulanon, Burks et al. 2013).

In situation where a disease may be limited to relatively small patches, such as would be the case during the early stages of infestation with a soil born disease, segmentation can help to identify potential areas, and therefore reduce the number of samples needed to detect its presence (Hillnhütter and Mahlein 2008). Early detection of diseases such as clubroot or Verticillium may allow for management options to contain their spread within the affected fields. Armed with a list of coordinates of potentially infested areas a field scout could survey for the presence of symptoms on canola stubble in a fairly efficient

manner without having to cover the whole field or limit the surveying to strategic points, such as the field entrance.

When patches are large enough to be readily visible on an image displayed at full extent and the patches are small in number, there is probably no need for an automated analysis. In these situations an experienced person will be able to interpret the image more accurately and more rapidly than can be done with current algorithms. The strength of the computational approach is the ability to process large amounts of visual information in a very detailed manner. Consider that an image of a quarter section captured at a resolution of 5 cm ground distance per pixel will contain 280 million data points per channel. When zoomed to 100 % (i.e. all pixels displayed) a regular HD monitor will only cover about 0.75 percent of the image, which makes the detailed visual inspection for crop scouting purposes impractical.

Indices calculated from spectral bands, such as the NDVI, are often used to classify pixels based on correlations with ground level observations. For reasons that have to do with scale and the varying spectral quality of incident light, these correlations often lack the robustness needed to reliably identify vegetation characteristics across different data sets. In a study on wheat rust, one author concluded that vegetation indices, including the NDVI, were generally poor predictors of disease severity (Ashourloo, Mobasheri et al. 2014). Good performance of the classification based on the indices was only obtained for low level foliar infections rated between 5-10%. Errors increased substantially for infection rates outside of this range. This suggests that a combination of spectral and object based analysis is needed. The latter would of course require even higher resolution images, which would have to be targeted to areas that are most likely to present symptoms.

Economic analysis

Cost of Conventional Field Scouting in southern Alberta

Methodology

Consultants and farmers employing consultants were contacted to provide prices for services as well as a summary of services provided. A total of five consulting service providers were interviewed covering an area bounded by Calgary on the west, Oyen at the north east, and Granum in the south west.

Findings

The cost of conventional field scouting in southern Alberta for traditional crops is in a very narrow range and the most common charge is $4.00 per acre. This price is based on a farm size in the order of 1500 acres or more. Field scouts surveyed indicated that the upper limit on the number of acres that could be scouted is about 20,000 acres for a scout with one assistant. The number of crops was not limited, but the farms surveyed produced a maximum of five cash crops. Irrigated field scouting is based on the same price for crops not requiring any special additional activities. Potatoes are the only crop identified as having a higher cost. The cost of field scouting for potatoes was not determined.

Services provided were also quite consistent. Field scouts would spend an average of five days on field scouting during the growing season and provide specific recommendations and advice on the use of seed varieties, fertilizer, chemicals as well as ongoing feedback to famers on the best practices regarding

the production of crops. Scouting activities include the identification of weeds and diseases that are or could result in yield loss.

Unmanned Aerial Vehicle Mapping Cost

Methodology

Two service providers in southern Alberta were contacted to determine cost and services provided. One service provider was able to provide images and information on cost of services. Research on technology available from interviews with service providers as well as publicly available information on unmanned vehicle hardware and software costs was collected. The information was used to estimate the operating costs of a farm owned UAV.

Findings

Current services in southern Alberta for agriculture consist of fixed wing air frames equipped with on board camera(s). Prices charged for generating an orthoimage of a field range from $3.00 to $4.00 per acre, depending on the volume of work. For this price the provider generally also includes an NDVI version of the field image. However the price does not include any interpretation or agronomic

Table 4. Cost estimate of operating a farm owned UAV on the basis of providing aerial images of 2000 acres 12 times during a cropping cycle. The cost do not include ground truthing, interpretation of the imagery, or the development of agronomic prescriptions.

	Estimate of on farm UAV operating cost to map 2000 acres per year		
	Total Cost	**Percent allocated to UAV**	**Cost allocated to UAV**
Interest on investment	$1,688	37 %	$624
Depreciation on UAV (3-year life cycle)	$6,600	100 %	$6,600
Depreciation on vehicle	$12,800	10 %	$1,280
Equipment insurance	$2,025	20 %	$405
Liability insurance	$2,000	10 %	$200
Communications (data and analogue)	$2,200	10 %	$220
Training, Regulatory and Travel	$2,800	100 %	$2,800
Casual labour	$2,880	100 %	$2,880
Fixed operating costs			$15,009
Operating and fixed cost per acre farmed			$7.50
Operating and fixed cost per acre mapped (one set of maps per week for 12 weeks, which corresponds 24,000 acres)			$0.63

prescription generated from the image. Fixed annual operating costs for a farm owned UAV were estimated at $15,000 per year (Table 4). For a 2000 acre farm the cost per acre would $7.50. Since multiple field images are needed to fully utilize the information that can be obtained from aerial images the cost per acre captured will be lower. For example, if twelve sets of images are captured the cost per acre would be only $0.63, which is of course much below the $3.00 per acre that specialized UAV operators are likely to charge. However the cost estimate for a farm owned and operated UAV does not include compensation of the owner's time needed to keep up with this rapidly developing technology and supervising an additional operation during an already busy field season. Furthermore one should also consider that, although largely automated, the operation and supervision of a UAV requires knowledge and compliance with the laws that regulate airspace. In practice this means that the person responsible for the UAV must obtain the necessary clearances, such as a Special Flight Operating Certificate for a specified location and time, as well as communicate with nearby airports and pilots sharing the airspace to inform them about the flight plans.

Expected Cost of UAV assisted Field Scouting

The following summarizes the estimated costs for a field scouting service supplemented with aerial imagery acquired with a UAV. Currently there is no such service provider operating in Southern Alberta.

Findings

A farmer owned UAV is estimated to cost $7.50 per acre, based on allocated fixed operating costs of $15,009 per year. For a 2000 acre farm where each field is captured 12 times during the cropping cycle the cost per acre would be $0.63.

If an UAV map is provided once a week for an arbitrary 12 weeks and cost is $3.00 per acre, then total cost for the aerial mapping would be $36 per acre. With the farmer collecting his own images and making them available to the field scouting service provider, the cost of acquiring the images could be considerably less, estimated at $7.50/acre for a set of 12 field images (Table 5).

Considering that time required to inspect fields is a major constraint for scouts, the use of aerial images may be very helpful, especially in view of new developments in precision farming. The current crop management model, where each field is treated as a more or less homogenous unit for the purpose of crop protection, will most likely be superseded by a model that operates on the basis of knowledge of the spatial heterogeneity within fields. Consequently there will be a growing expectation that field scouts can deliver this kind of information, which will include maps that can be readily loaded into the navigation systems of farm equipment. Once the aerial monitoring and mapping of crop performance becomes a regular part of crop production, the ability to store and analyze this information will greatly enhance its value. There is little doubt that the next generation of crop consultants will need to have the skills to work with large amounts of spatial data that may be obtained from a variety of sources, such as UAVs, satellites, yield monitors etc. For farmers the benefits of early adoption may not be immediately apparent, but will certainly make a difference over the longer term, because of their enhanced ability to position their enterprise to take advantage of new variable rate seeding and spraying technology as it becomes available.

Table 5. Cost comparison of UAV assisted custom field scouting, where the aerial images and derived products (e.g. NDVI field image) is either fully contracted out or where only the field scouting is contracted out with the farmer supplying the aerial images at cost and without charging for labour.

	Fully contracted UAV Assisted Field Scouting	**Custom Field Scouting with farm supplied UAV imagery**
Custom Field Scouting	$4.00/acre	$4.00/acre
UAV aerial imagery (12 sets)	$36.00/acre	$7.50/acre
Total cost per acre	$40.00/acre	$11.50/acre

Comparison of the Cost of Crop Protection Inputs and the Cost of UAV Assisted Field Scouting

Methodology

Consultants, farmers, and input providers were contacted to provide a summary of crop weed and disease control practices in Southern Alberta. Estimates of crop protection costs were based on prices charged in 2015, as determined by interviewing producers and input providers in an area bounded by Calgary on the west, Oyen at the north east, and Granum in the south west.

Findings

As shown in table 6, the cost of crop protection varies considerably between crops. The crops with the lowest cost are barley and spring wheat, followed by canola, field peas, seed alfalfa and finally potatoes. Of course not all items are equally important for all crops. For example weed control is much higher in potatoes and seed alfalfa then it is in the other crops. However, in practice these costs can fluctuate considerable as a result of new pests or the need to use a more expensive control product because of pest resistance to cheaper products. For example with herbicide resistant weed, farmers may have to switch to multiple more expensive products, where a single low cost product would have previously done the job.

The cost of UAV assisted field scouting can be expected to be three to ten times the cost of conventional field scouting (Table 5). At the highest estimated cost, $40/acre, it would correspond to 44% of the cost of crop protection in barley or spring wheat, 37% in canola, 30% in field peas, 10% in potatoes and 25% in seed alfalfa. There should be a substantial net gain to justify this expense, which is probably most readily achieved in crops with the highest crop protection costs.

With respect to crop protection this technology is most likely to provide satisfactory economic returns where variable rate applications make sense (uneven distribution of a relatively immobile pest) or where the analysis of the imagery can lead to early detection of a pest that has the potential to severely reduce crop yield and/or future crop options if allowed to spread. Examples of the latter are clubroot in canola or late blight in potatoes.

Table 6. Per acre cost estimates of crop protection inputs for selected crops in Southern Alberta. The estimate include the cost of application based on average rates charged by custom applicators.

Crop Protection Item	Barley	Spring Wheat	Canola	Field Peas	Potatoes	Seed Alfalfa
Pre-emergence weed control	$15	$15	$15	$15		
Post-emergence weed control	$32	$32	$39	$39	$67	$71
Inoculant				$9		
Seed treatment	$8	$8		$16	$70	
Insect control			$17	$17	$17	$54
Disease control	$37	$37	$37	$37	$230	$37
Total (per acre cost)	$92	$92	$108	$133	$384	$162

Conclusion

Early season weed scouting:

- The resolution of the aerial images obtained (6 cm GSD) was too coarse to assess weed density early in the season.
- A GSD of 6 cm (1 pixel corresponds to 6 cm by 6 cm on the ground) results in images where pixels covering small weeds are often not distinguishable from soil or other background that is not living plant material. Capturing images at higher resolutions is possible, but is not practical because of the very large amount of data that would have to be processed and managed.
- As an alternative to whole field image mosaics we showed that it is possible to extract information on weed density by removing crop rows from images captured at a much higher resolution and calculate weed density on the basis of vegetation found between crop rows. In this way a weed density map can be constructed without the need to first generate an image of the entire field.

Disease detection in crops:

- The resolution of aerial images obtained was adequate to clearly locate areas as small as one square meter.
- Segmentation algorithms can be effective in locating areas within crops that exhibit patterns that may be associated with certain diseases.
- Automated pattern detection can be especially useful where the affected areas are small and would otherwise require time consuming visual searches of large images.
- Aerial images captured with UAVs are a new tool for the early detection of crop diseases.

Economic feasibility:

- The addition of UAV acquired aerial images to regular crop scouting services, where each service is contracted to a separate provider, would drastically increase the cost and therefore could only be considered in high value crops, such as potatoes.
- UAV acquired aerial images could be produced at a much lower cost if done by farm owned and operated equipment, as opposed to a contracted service.

Cited Literature

Ashourloo, D., M. R. Mobasheri and A. Huete (2014). "Evaluating the effect of different wheat rust disease symptoms on vegetation indices using hyperspectral measurements." Remote Sensing **6**(6): 5107-5123.

Baranowski, P., M. Jedryczka, W. Mazurek, D. Babula-Skowronska, A. Siedliska and J. Kaczmarek (2015). "Hyperspectral and thermal imaging of oilseed rape (Brassica napus) response to fungal species of the genus Alternaria." PLoS ONE **10**(3): e0122913-e0122913.

Bulanon, D. M., T. F. Burks, D. G. Kim and M. A. Ritenour (2013). "Citrus black spot detection using hyperspectral image analysis." Agricultural Engineering International: CIGR Journal **15**(3): 171-180.

Clark, E. E. (1990). "Aerial photography in the control of crop disease." Chemistry and Industry (London)(8): 250-253.

Dlouhy, M., J. Lev and M. Kroulik (2016). "Technical and software solutions for autonomous Unmanned Aerial Vehicle (UAV) navigation in case of unavailable GPS signal." Agronomy Research **14**(3): 733-744.

Evans, N., A. Baierl, P. Brain, S. J. Welham and B. D. L. Fitt (2003). "Spatial aspects of light leaf spot (Pyrenopeziza brassicae) epidemic development on winter oilseed rape (Brassica napus) in the United Kingdom." Phytopathology **93**(6): 657-665.

Gold, H. J., G. G. Wilkerson and J. Bay (1996). "Scouting for weeds, based on the negative binomial distribution." Weed science **44**(3): 504-510.

Hillnhütter, C. and A. K. Mahlein (2008). "Early detection and localisation of sugar beet diseases: new approaches. / Neue Ansätze zur frühzeitigen Erkennung und Lokalisierung von Zuckerrübenkrankheiten." Gesunde Pflanzen **60**(4): 143-149.

Isard, S. A. and M. Chamecki (2016). "A physically based theoretical model of spore deposition for predicting spread of plant diseases." Phytopathology **106**(3): 244-253.

Krueger, D. W., G. G. Wilkerson, H. D. Coble and H. J. Gold (2000). "An economic analysis of binomial sampling for weed scouting." Weed Science **48**(1): 53-60.

Peña-Barragãn, J. M., A. I. d. Castro-Mejías, J. Torres-Sánchez and F. López-Granados (2013). Multispectral images captured by an unmanned aerial vehicle (UAV): a technological innovation for weed mapping in early-season. / Imágenes multiespectrales procedentes de un vehículo aéreo no tripulado (UAV): una innovación tecnológica para la detección de malas hierbas en fase temprana. XIV Congresso de la Sociedad Española de Malherbología, Valencia, España, 5 al 7 de noviembre de 2013. J. M. O. Lluch, D. G. d. Barreda Ferraz, V. C. Zeising and N. P. Seva. València; Spain, Universitat Politècnica de València**:** 49-53.

Rasmussen, J., G. Ntakos, J. Nielsen, J. Svensgaard, R. N. Poulsen and S. Christensen (2016). "Are vegetation indices derived from consumer-grade cameras mounted on UAVs sufficiently reliable for assessing experimental plots?" European Journal of Agronomy **74**: 75-92.